Gait deviation and neurological diseases: a comparative study of quantitative measures

Lorenzo Hermez, Nesma Houmani, Sonia Garcia-Salicetti, Omar Galarraga, Vincent Vigneron

Gait Deviation and Neurological Diseases: a comparative Study of Quantitative Measures

Lorenzo Hermez[1[0009-0000-5974-9428]], Nesma Houmani[1*[0000-0002-5048-9313]], Sonia Garcia-Salicetti[1[0000-0001-5257-8216]], Omar Galarraga[2[0000-0002-5564-7624]], Vincent Vigneron[3[0000-0001-5917-6041]]

[1]SAMOVAR, Télécom SudParis, Institut Polytechnique de Paris, 91120 Palaiseau, France
[2]Movement Analysis Laboratory, UGECAM Ile-de-France, 77170 Coubert, France
[3]Informatique, Bio-Informatique et Systèmes Complexes (IBISC) EA 4526, Université Paris-Saclay, 91020 Evry, France

Abstract. This comparative study addresses the quantification of gait deviations from normal gait, and across different motor impairments induced by neurological diseases. We compared Gait Deviation Index and Gait Profile Score, well-known in the literature, to a novel 3D-metric based on Dynamic Time Warping (DTW). These deviation measures are analyzed following the same methodology, based on unsupervised learning, on the same database. Results show that our 3D-metric outperforms the others. This confirms that for finely quantifying deviations, it is crucial to consider different references to represent normal gait variability, as well as using an elastic distance (DTW) for matching two gait cycles.

Keywords: Gait Deviation Index · Gait Profile Score · Normal Gait Profiles · Dynamic Time Warping · Knee Angular Kinematics

1 Introduction

Gait, the coordinated series of movements that allow humans to move from one place to another, is a fundamental aspect of our daily lives. The study of gait has deep implications for various fields, including biomechanics, rehabilitation, sports science, and robotics. Recent advances in sensor technology, such as inertial measurement units (IMUs) [1–5] and motion capture systems [6, 7], have made it possible to collect high-resolution angular data from multiple joints simultaneously [1, 8–11]. Clinical Gait Analysis (CGA) exploits such sequences describing gait, for decision aid to clinicians [12, 13]. In the framework of gait rehabilitation, quantitative measures are necessary to assess the progress of a patient during a therapy. Several works in the literature tackle this field and different measures have been proposed up to now [13]. One of the most widely used is the Gait Deviation Index (GDI) [14] among others, such as the Gait Profile Score (GPS) [15] and Gillette Gait Index (GGI) [16]. The objective of such measures is to quantify the deviation from the normal gait pattern.

Ideally, a well-defined gait deviation measure should be able to detect abnormal gait and also to characterize the intensity of the deviation. With this particular focus, in this paper, we study comparatively the GDI and a new measure that we have recently proposed [17]. In particular, our aim is to evaluate what exactly each measure quantifies on a same dataset. We perform this analysis on patients suffering from neurological diseases (Cerebral Palsy, Traumatic Brain Injury, Spinal Cord Injury, Stroke, or Multiple Sclerosis), who are followed at the Movement Analysis Laboratory of Coubert Rehabilitation Center, at UGECAM Ile-de-France.

In order to measure gait deviations, the first step is to define a good reference for normal gait. This crucial aspect has been tackled in different ways in the literature. The most common paradigm to define a normal gait reference is to average normalized gait cycles (usually into 51 points) belonging to all healthy subjects of a given dataset, as considered by the GPS [15]. Another option is to construct a universal space of gait features, based on both healthy and pathological subjects, and to average in such space the vectors corresponding to healthy subjects, as done by the GDI [14]. By contrast, we have proposed to represent normal gait by K reference cycles in order to take into account the natural variability of gait in the healthy population [17]. Of note, the GDI considers the "universal" variance of gait in both healthy and pathological populations.

In order to measure gait deviations from normal gait, the second step is to define the metric. Usually, the literature exploits the Euclidean distance [14, 15]. We have compared it to an elastic distance, namely Dynamic Time Warping (DTW), and showed that DTW is better suited for comparing gait cycles [17].

In this work, we will analyze the differences and relative contributions of the above-mentioned works, on the Coubert Rehabilitation Center (CRC) dataset. In particular, we will assess, with a common methodology, the different gait deviation measures, in terms of motor impairments induced by the neurological diseases: Hemiplegia, Paraplegia and Tetraplegia.

This paper is organized as follows. Section II presents the CRC dataset, describes the main approaches in the literature of gait deviations, and the methodology used to compare them. Results are given in Section III. Conclusions and perspectives are stated in Section IV.

2 Database and Methods

2.1 Database

We exploited angular kinematic data acquired during a spontaneous gait task in 52 healthy subjects and 38 patients suffering from neurological diseases. Data was collected at Movement Analysis Laboratory of Coubert Rehabilitation Center, at UGECAM Ile-de-France, using Codamotion optoelectronic system. The system recovers angle kinematics during walking for five joints (pelvis, hip, foot, ankle and knee) in three planes (sagittal, frontal and transverse), with a sampling rate of 100 Hz.

The recruited healthy subjects were young adults with no motor function impairment (see Table I).

Table 1. Descriptive statistics of our dataset

	Healthy subjects	**Pathological patients**
Number of patients	52	38
Female	34	13
Age (mean ± std)	22.62 ± 3.89 (y.o)	46.82 ± 12.93
Height (mean ± std)	1.71 ± 0.09 (m)	1.70 ± 0.10
Weight (mean ± std)	65.28 ± 10.77 (kg)	71.06 ± 13.99
Speed (mean ± std)	1.20 ± 0.14 (m/s)	0.52 ± 0.24

Patients were followed-up at the Coubert Rehabilitation Center for motor problems caused by neurological diseases (Cerebral Palsy, Traumatic Brain Injury, Spinal Cord Injury, Stroke, or Multiple Sclerosis). These diseases are often the cause of motor impairments affecting one or more limbs of the upper and/or lower body: Hemiplegia (HP), Tetraplegia (TP) or Paraplegia (PP). We have 18 HP patients, 11 TP patients and 9 PP patients.

2.2 Preprocessing

The angular kinematics of each joint, captured during each gait trial, is a periodic signal consisting of different consecutive cycles, defined between the initial contact event and the terminal swing event (see Figure 1.a). This signal was segmented into gait cycles, automatically detected with the High-pass algorithm [18] and controlled by an expert (see Figure 1.b).

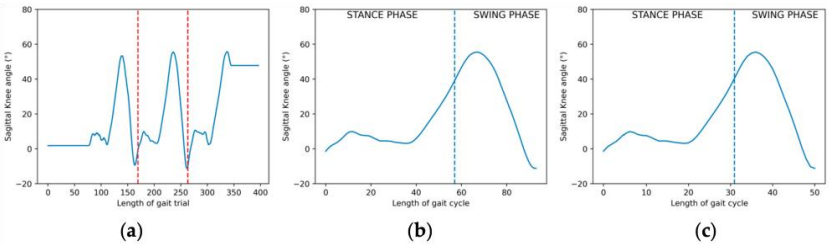

Fig. 1. Knee angular kinematics in the sagittal plane: (a) a periodic sequence of one trial; (b) a raw segmented knee cycle; (c) the normalized segmented knee cycle. Red dotted lines define the beginning and end of a gait cycle.

We focused on the analysis of the knee joint kinematics in the sagittal plane only. Gait cycles are normalized into 51 points, as shown in Figure 1.c. The number of cycles was not the same for all trials and differed for each patient. The total number of knee sagittal cycles used is 872 cycles: 526 cycles belong to healthy subjects, 162 for HP, 106 for TP, and 78 for PP patients.

2.3 Gait Deviation Index (GDI)

This index exploits Singular Value Decomposition (SVD) performed on gait data including the normalized angular kinematics (into 51 points) of 9 angles simultaneously: pelvic and hip angles in sagittal, frontal and transversal planes, knee and ankle angles in sagittal plane and foot in transversal plane. Thus, each subject is represented by a gait vector g of 459 dimensions (51 points x 9 angular kinematics). SVD is performed on vectors of both healthy and pathological populations, to obtain singular vectors F_k, called gait features. In this framework, m singular vectors are used to reconstruct gait vectors, according to (1):

$$\tilde{g}^m = \sum_{k=1}^{m} c_k . F_k \quad where \quad c_k = < g ; F_k > \tag{1}$$

The deviation is then given by:

$$GDI^{\alpha}{}_{raw} = ln\left(\left|\left|c^{\alpha} - \overline{c}_{TD}\right|\right|_2\right) \tag{2}$$

The gait deviation index is then obtained as follow:

$$GDI = 100 - 10\, zGDI^{\alpha}{}_{raw} \tag{3}$$

$$where \qquad zGDI^{\alpha}{}_{raw} = \frac{zGDI^{\alpha}{}_{raw} - Mean\left(\{GDI^{k}{}_{raw}\}_{k\in TD}\right)}{STD\left(\{GDI^{k}{}_{raw}\}_{k\in TD}\right)} \tag{4}$$

2.4 Our Methodology

As in [17], we apply the unsupervised K-Medoids (K=3) on all healthy cycles, to retrieve normal gait references, called "Normal Gait Profiles" (NGPs). This method allows finding real representatives, i.e. gait cycles belonging to individuals in the dataset. The classical version of *K*-Medoids usually exploits the Euclidean distance as a dissimilarity metric. However, this distance does not take into account time shifts of similar patterns when comparing two cycles [17]. To overcome these limitations, we integrated in the *K*-Medoids algorithm an elastic distance, namely Dynamic Time Warping (DTW) [19]. DTW relies on finding the best warping path to assign two time signals, by minimizing the cumulative distance between the assigned points in the two signals. This distance has been used in gait analysis [20] and more recently to measure gait symmetry [21, 22]. Then, we studied the deviation of pathological gait cycles from the obtained NGPs, according to the three types of motor impairments. Each gait cycle is characterized by a 3D vector, composed of the cycle's DTW distances to the three NGPs. In an attempt to stratify deviations from NGPs, we applied Agglomerative Hierarchical Clustering (AHC) using Ward's linkage function [23]. This algorithm makes it possible to analyze the deviations across different clusters (in this case 3 clusters), thereby suggesting three degrees of severity among pathological cycles. The methodology is presented in detail in [17].

3 Results

3.1 Our Approach

We applied *K*-medoids by fixing K = 3 to consider two extreme behaviors and one intermediate one. Figure 2 shows the three NGPs (medoids) on 51 points.

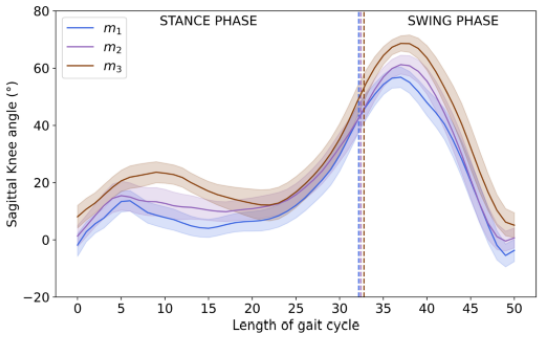

Fig. 2. The three NGP (cycles) representing healthy subjects in our dataset, extracted with the *K*-medoids algorithm.

We notice that the three NGPs capture the diversity present in the healthy population, particularly in the stance phase: during the loading response [24], the three NGPs show variability as well as time shifts between one another (see Figure 2). This reflects the potential of DTW for time-aligning two signals at important transitions. On the other hand, Table II shows, through the metadata of the three NGPs, this diversity of the healthy population, especially in height, weight and speed.

Table 2. Metadata associated with the three NGP

NGP	Gender	Age (y.o)	Height (m)	Weight (kg)	Speed (m/s)
NGP 1	F	20	1.61	65.0	1.23
NGP 2	F	27	1.66	64.7	1.00
NGP 3	M	22	1.83	68.1	1.17

As explained in Section II.D, we perform AHC in the 3D space, to investigate the potential of such 3D-metric to finely quantify gait deviations according to different pathologies (HP, PP and TP). Figure 3 displays the distribution of cycles per person in clusters. Each person is represented by a vertical bar, accounting for the number of cycles of this person in each cluster. A color code is used for a better visualization of the deviations: green gait cycles are the closest to healthy gait, red cycles are the most distant, and orange cycles have an intermediate behavior. For a better readability, healthy controls (HC) are grouped on the left and patients are grouped by motor impairment on the right, sorted as follows: Hemiplegia (HP), Paraplegia (PP) and Tetraplegia (TP).

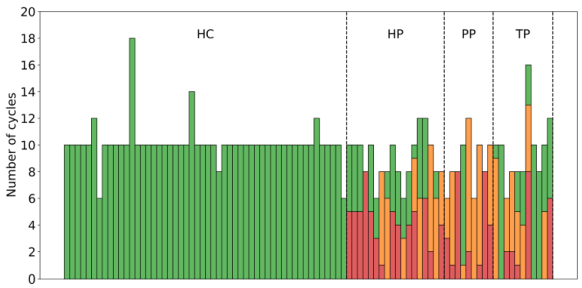

Fig. 3. Distribution of cycles per person (a bar represents one person) within the three clusters. Cycles in green are the closest to NGPs, followed by cycles in orange and then in red (the most distant to NGPs). Persons are grouped according to their class: HCs for healthy controls, HP for Hemiplegic, PP for Paraplegic and TP for Tetraplegic patients.

We notice in Figure 3 that all healthy cycles are grouped into the closest cluster to the NGPs (green cluster). On the other hand, we observe different distributions in clusters between motor impairments (HP, PP, TP). On HP patients, most patients have their cycles assigned to two clusters: 13 HP patients among the 18 have some of their cycles in the green cluster and the remaining ones are mostly in the red cluster. This is in accordance with the lateral impact of Hemiplegia: the healthy side is close to the NGPs (green cluster), whereas the cycles of the impacted side are considered as being strongly (red) or slightly (orange) impacted. For PP patients, most of their cycles are assigned to the orange (intermediate) cluster. Only two patients have all their cycles assigned to the red one. Finally, as TP patients have incomplete Tetraplegia, we observe more cycles assigned to the green cluster comparatively to PP patients.

These results show the effectiveness of the proposed 3D-metric in finely quantifying gait deviations from healthy gait according to each specific pathology.

3.2 Comparative Analysis with GDI and GPS

We computed GDI considering the 9 angular kinematics for all cycles, as explained in Section II.C. For the purpose of comparing our 3D-metric to the GDI, we performed an AHC on the obtained GDI values.

Figure 4 displays the distribution of GDI values per cluster after performing AHC. We display in green the cluster containing the cycles with highest GDI, in red the cluster containing the cycles with lowest GDI, and in orange the intermediate one. We notice that the green cluster, representing the closest cycles to normal gait, gather GDI values around 100 or higher, as expected.

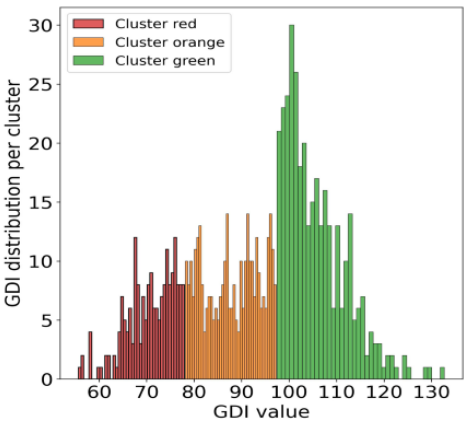

Fig. 4. GDI distribution per cluster after performing AHC.

Figure 5 shows the distribution of cycles per person in the three resulting clusters based on GDI.

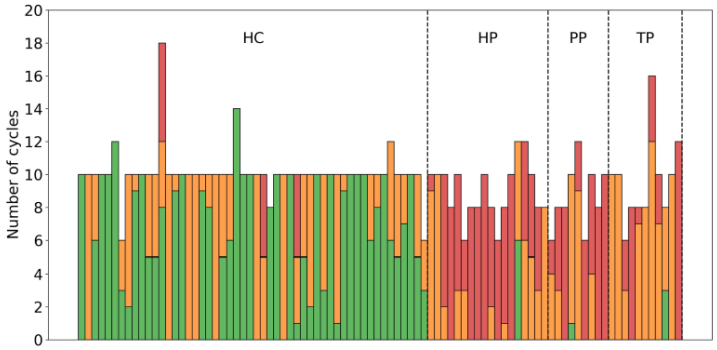

Fig. 5. Distribution of cycles per person after AHC based on GDI values calculated on 9 angular kinematics.

When comparing the distribution of cycles with GDI (Figure 5) and that with our 3D-metric (Figure 3), we first notice that, with GDI, most HP patients have their cycles in the red cluster, thereby losing the distinction between the impacted and nonimpacted sides. Also, almost all TP cycles are in the orange cluster, with intermediate GDI values, as we can expect for incomplete TP patients. However, there is no specific trend in both HP and PP. We conclude that GDI is not precise enough to characterize these motor impairments in terms of gait deviation.

We propose to compute the GDI values considering only the knee angular kinematics as our 3D-metric. Figure 6 reports the results in the three clusters. There is no distinctive trend between motor impairments: almost all pathological cycles are assigned to the red cluster. All these results highlight that our 3D-metric outperforms the GDI in finely quantifying gait deviations from normality.

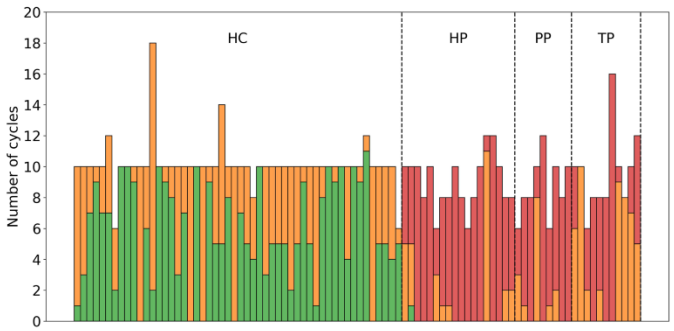

Fig. 6. Distribution of cycles per person after AHC based on GDI values calculated on knee angular kinematics.

For a complete comparison, we also computed the GPS on the same data (only the knee joint), considering as reference the average cycle of all the healthy cycles as in [15]. Figure 7 shows that GPS is highly correlated to GDI, as found in [14], with the same exponential trend.

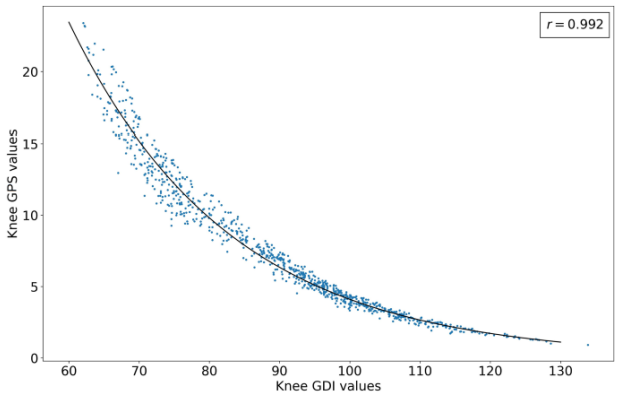

Fig. 7. GPS as a function of GDI on the knee joint.

4 Conclusions

This study has the objective to quantify gait deviations from normality and to characterize deviation trends across different motor impairments related to neurological diseases. Our proposed 3D-metric was compared to the GDI and GPS on the CRC dataset. Results demonstrate the potential of our 3D-metric in characterizing finely gait deviations, although only the knee joint has been exploited up to now. The effectiveness of our approach relies on one hand, on constructing a normal gait reference that takes into account gait variability in the healthy population. On the other hand, the DTW metric for measuring deviations is suited to match cycles showing temporal shifts.

In future work, we will extend our approach considering the other joints' angular kinematics and study which joints are more pertinent to characterize each motor impairment.

References

1. Błażkiewicz, M., Wit, A.: Artificial neural network simulation of lower limb joint angles in normal and impaired human gait. Acta of bioengineering and biomechanics. **20**, pp. 43–49 (2018). doi:10.5277/ABB-00367-2018
2. Luu, T.P., Low, K.H., Qu, X., Lim, H.B., Hoon, K.H.: An individual-specific gait pattern prediction model based on generalized regression neural networks. Gait & posture. **39**, pp. 443–448 (2014). doi:10.1016/j.gaitpost.2013.08.020
3. Sivakumar, S., Gopalai, A.A., Lim, K.H., Gouwanda, D.: Artificial neural network-based ankle joint angle estimation using instrumented foot insoles. Biomedical Signal Processing and Control. **54**, 101614 (2019). doi:10.1016/j.bspc.2019.101614
4. Renani, M.S., Eustace, A.M., Myers, C.A., Clary, C.W.: The use of synthetic IMU signals in the training of deep learning models significantly improves the accuracy of joint kinematic predictions. Sensors. **21**, 5876 (2021). doi:10.3390/s21185876
5. Stetter, B.J., Krafft, F.C., Ringhof, S., Stein, T., Sell, S.: A machine learning and wearable sensor-based approach to estimate external knee flexion and adduction moments during various locomotion tasks. Frontiers in bioengineering and biotechnology. **8**, (2020) doi:10.3389/fbioe.2020.591876
6. Giarmatzis, G., Zacharaki, E.I., Moustakas, K.: Real-time prediction of joint forces by motion capture and machine learning. Sensors. **20**, 6933 (2020). doi:10.3390/s20236933
7. Wouda, F.J., Giuberti, M., Bellusci, G., Veltink, P.H.: "Estimation of full-body poses using only five inertial sensors: an eager or lazy learning approach?" Sensors. **16**, 2016, 2138 (2019). doi:10.3390/s16122138
8. Argent, R., Drummond, S., Remus, A., O'Reilly, M., Caulfield, B.: Evaluating the use of machine learning in the assessment of joint angle using a single inertial sensor. Journal of rehabilitation and assistive technologies engineering. **6**, (2019).
9. Chen, J., Zhang, X., Cheng, Y., Xi, N. (2018).: Surface EMG-based continuous estimation of human lower limb joint angles by using deep belief networks. Biomedical Signal Processing and Control. 40, pp.335–342 (2018). doi: 10.1016/j.bspc.2017.09.013
10. Farmer, S., Silver-Thorn, B., Voglewede, P., Beardsley, S.A.: Within-socket myoelectric prediction of continuous ankle kinematics for control of a powered transtibial prosthesis. Journal of neural engineering. **11**, 056027 (2014). doi: 10.1088/1741-2560/11/5/056027
11. Findlow, A., Goulermas, J.Y., Nester, C., Howard, D., Kenney, L.P.J.: Predicting lower limb joint kinematics using wearable motion sensors. Gait & posture. **28**, pp. 120–126 (2008). doi:10.1016/j.gaitpost.2007.11.002
12. Zeng, W., Yuan, C., Wang, Q., Liu, F., Wang, Y.: Classification of gait patterns between patients with Parkinson's disease and healthy controls using phase space reconstruction (PSR), empirical mode decomposition (EMD) and neural networks. Neural Networks. **111**, pp. 64–76 (2019). doi:10.1016/j.neunet.2018.12.007
13. Cimolin, V., Galli, M.: Summary measures for clinical gait analysis: a literature review. Gait Posture. **39**, pp. 1005–1010 (2014). doi:10.1016/j.gaitpost.2014.01.085

14. Schwartz, M.H., Rozumalski, A.: The gait deviation index: a new comprehensive index of gait pathology. Gait Posture. **28**, pp. 351–357 (2008). doi:10.1016/j.gaitpost.2008.02.005
15. Baker, R., McGinley, J.L., Schwartz, M.H., et al.: The gait profile score and movement analysis profile. Gait Posture. **30**, pp. 265–269 (2009). doi:10.1016/j.gaitpost.2009.05.018
16. Cretual, A., Bervet, K., Ballaz, L.: Gillette gait index in adults. Gait Posture. **32**, pp. 307–310 (2010). doi:10.1016/j.gaitpost.2010.05.020
17. Hermez, L., Halimi, A., Houmani, N., et al.: Clinical gait analysis: characterizing normal gait and pathological deviations due to neurological diseases. Sensors. **23**, 6566 (2023). doi: 10.3390/s23236566
18. Desailly, E., Daniel, Y., Sardain, P., Lacouture, P.: Foot contact event detection using kinematic data in cerebral palsy children and normal adults gait. Gait Posture. **29**, pp. 76–80 (2009). doi: 10.1016/j.gaitpost.2008.07.015
19. Sakoe, H., Chiba, S.: Dynamic programming algorithm optimization for spoken word recognition. IEEE Transactions on Acoustics, Speech, and Signal Processing. **26**, pp. 43–49 (1978). doi:10.1109/TASSP.1978.1163055
20. Zhao, H., Xu, H., Wang, Z., et al.: Analysis and evaluation of hemiplegic gait based on wearable sensor network. Information Fusion. **90**, pp. 382-391 (2023). doi:10.1016/j.inffus.2022.06.012
21. Błażkiewicz, M., Lann Vel Lace, K., Hadamus, A.: Gait Symmetry Analysis Based on Dynamic Time Warping. Symmetry. **13**, pp. 836 (2021).
22. Wang, X., Kyrarini, M., Ristić-Durrant, D., et al.: Monitoring of gait performance using dynamic time warping on IMU-sensor data. IEEE International Symposium on Medical Measurements and Applications (MeMeA). pp. 1-6 (2016).
23. Ward, J.H.: Hierarchical grouping to optimize an objective function. Journal of the American Statistical Association. **58**, pp. 236–244 (1963).
24. Bonnefoy-Mazure, A., Armand, S.: Orthopedic Management of Children with Cerebral Palsy. Nova Science Publishers (2015).